The Journal of Neuroscience, March 15, 2001, 21(6):1884–1892

Recovery from Inactivation of T-Type Ca^{2+} Channels in Rat Thalamic Neurons

Chung-Chin Kuo[1,2] **and Shibing Yang**[1]

[1]*Department of Physiology, National Taiwan University College of Medicine, and* [2]*Department of Neurology, National Taiwan University Hospital, Taipei 100, Taiwan*

We studied the gating kinetics, especially the kinetics of recovery from inactivation, of T-type Ca^{2+} channels (T-channels) in thalamic neurons. The recovery course is associated with no discernible Ca^{2+} current and is characterized by an initial delay, as well as a subsequent exponential phase. These findings are qualitatively similar to previous observations on neuronal Na^+ channels and suggest that T-channels also must deactivate to recover from inactivation. In contrast to Na^+ channels in which both the delay and the time constant of the exponential phase are shortened with increasing hyperpolarization, in T-channels the time constant of the exponential recovery phase remains unchanged between −100 and −200 mV, although the initial delay is still shortened *e*-fold per 43 mV hyperpolarization over the same voltage range. The deactivating kinetics of tail T-currents also show a similar voltage dependence between −90 and −170 mV. According to the hinged-lid model of fast inactivation, these findings suggest that the affinity difference between inactivating peptide binding to the activated channel and binding to the fully deactivated channel is much smaller in T-channels than in Na^+ channels. Moreover, the inactivating peptide in T-channels seems to have much slower binding and unbinding kinetics, and the unbinding rates probably remain unchanged once the inactivated T-channel has gone through the initial steps of deactivation and "closes" the pore (with the activation gate). T-channels thus might have a more rigid hinge and a more abrupt conformational change in the inactivation machinery associated with opening and closing of the pore.

Key words: T-type Ca^{2+} channel; activation; deactivation; inactivation; recovery from inactivation; gating

Fast inactivation is an important gating phenomenon in many voltage-gated ion channels, such as Na^+, Shaker K^+, and T-type Ca^{2+} channels (T-channels). Upon membrane depolarization, these channels are rapidly activated and then rapidly inactivated. Fast inactivation thus tightly controls ion flow through the channel. A classical mechanistic view of fast inactivation is the "ball-and-chain" model (Armstrong and Bezanilla, 1977; Armstrong, 1981), in which inactivation results from blockade of the activated channel pore by part of the channel protein (such as the N terminal region in Shaker K^+ channels) (Hoshi et al., 1990; Zagotta et al., 1990). More recently, West et al. (1992) proposed a somewhat different "hinged-lid" model, in which the linker peptide between transmembrane domains III and IV of the Na^+ channel protein functions as a "lid" to control ion permeation at the internal pore mouth. Both models, however, are the same in postulating fast inactivation as open-channel blockade produced by binding of the inactivating peptide to a receptor uncovered or produced by channel activation.

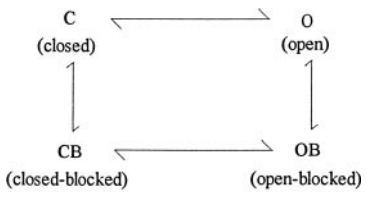

scheme 1

Scheme 1 is a simplified diagram incorporating the foregoing concepts of fast inactivation, in which OB and CB denote the open (activated) and closed (deactivated) conformations blocked by the inactivating peptide, respectively. In principle, route C to O to OB is the major (or even exclusive) pathway for the development of inactivation, so that inactivation is coupled to activation. On the other hand, the inactivated channel (state OB) may recover through the OB to O to C (unblocking-first) route or the OB to CB to C (deactivation-first) route. The unblocking-first route implies substantial ionic current through the channels traversing state O during recovery. The deactivation-first route ensures no such currents, but the recovery time course might be characterized by a voltage-dependent initial delay that corresponds to deactivation of the inactivated channels (OB to CB step). Inactivated Na^+ channels always take the deactivation-first route to recover (Kuo and Bean, 1994), whereas recovery of inactivated Shaker K^+ channels favors the OB to O to C route (Kuo, 1997).

The molecular mechanisms underlying the development and recovery of fast inactivation in T-channels have been less extensively studied. The macroscopic inactivation rates of T-channels saturate at positive potentials (Chen and Hess, 1990; Herrington and Lingle, 1992; Serrano et al., 1999), indicating lack of intrinsic voltage dependence of the inactivation process itself. There is no obvious Ca^{2+} current associated with recovery of cloned (α1G) T-channels at −100 mV (Serrano et al., 1999). Also, there is an initial delay in the recovery time course of the cloned α1G and α1H channels at −100 mV (Satin and Cribbs, 2000). These findings would support the deactivation-first route of recovery. However, more rigorous examination of the initial delay and the current associated with recovery at different recovery potentials seems necessary, because the choice of recovery route may be different at different potentials (Kuo, 1997). The recovery kinetics

Received Oct. 23, 2000; revised Dec. 27, 2000; accepted Jan. 2, 2001.

This work was supported by National Science Council, Taiwan, Republic of China Grant NSC-89-2320-B-002-068.

Correspondence should be addressed to Chung-Chin Kuo, Department of Physiology, National Taiwan University College of Medicine, 1 Jen-Ai Road, First Section, Taipei 100, Taiwan. E-mail: cckuo@ha.mc.ntu.edu.tw.

of fibroblast or cloned (α1G) T-channels are voltage-independent between −100 to −130 mV but become slower at more positive potentials (Chen and Hess, 1990; Serrano et al., 1999). However, the recovery kinetics of T-channels in rat GH3 pituitary cells remain unchanged throughout −80 to −130 mV (Herrington and Lingle, 1992), suggesting different biophysical properties of T-channels in different tissues. We therefore studied the recovery of inactivated T-channels in thalamic neurons, in which T-channels play an essential role in controlling the discharge pattern (for review, see McCormick and Bal, 1997). We found that, like Na^+ channels, T-channels also take the deactivation-first route to recover from inactivation. However, the differential work it takes to deactivate the inactivated (state OB) and the open (state O) channels seems to be much smaller in T-channels than in Na^+ channels. Also, T-channels probably have a more rigid hinge and a more abrupt conformational change in the inactivation machinery associated with opening and closing of the pore.

MATERIALS AND METHODS

Cell preparation. Coronal slices of the whole brain were prepared from 8- to 12-d-old Wistar rats. The brain was cooled in 0°C cutting solution (125 mM sucrose, 20 mM Na_2SO_4, 10 mM K_2SO_4, 3 mM $MgCl_2$, and 10 mM HEPES, pH 7.4) for 1 min. The tissue block containing thalamus was then cut into 400 μm slices with a vibratome (Campden Instruments, Silbey, UK). The ventroposterior complex (including the ventroposterior medial and ventroposterior lateral nuclei) of thalamus was dissected from the slices and cut into small pieces. After treatment for 3–5 min at 33°C in dissociation medium (82 mM Na_2SO_4, 30 mM K_2SO_4, 0.4 mM $CaCl_2$, 3 mM $MgCl_2$, 5 mM HEPES, and 0.001% phenol red indicator, pH 7.4) containing 0.5 mg/ml trypsin (type XI; Sigma, St. Louis, MO), the tissue pieces were moved to dissociation medium containing no trypsin but 2 mg/ml bovine serum albumin (Sigma). Each time when cells were needed, two to three pieces were picked and triturated to release single neurons.

Whole-cell recording. The dissociated neurons were put in a recording chamber containing Tyrode's solution (150 mM NaCl, 4 mM KCl, 2 mM $MgCl_2$, 2 mM $CaCl_2$, and 10 mM HEPES, pH 7.4). Seal was formed, and whole-cell configuration was obtained in Tyrode's solution. The cell was then lifted from bottom of the chamber and moved in front of an array of flow pipes (content 1 μl, length 64 mm; Microcapillary; Hilgenberg Inc., Malsfeld, Germany) emitting different external solutions. The external solution for recording Ca^{2+} currents contains 150 mM tetraethylammonium chloride, 5 mM $CaCl_2$, 10 mM HEPES, and 3 μM tetrodotoxin, pH 7.4. Except for the experiments in Figure 1*A–D*, 1 μM nimodipine and 0.5 μM ω-conotoxin MVIIC were always added to the external solution to prevent contamination of T-current by L-, N-, and P/Q-type Ca^{2+} currents. Whole-cell voltage-clamp recordings were made using pipettes pulled from borosilicate micropipettes (outer diameter, 1.55–1.60 mm; Hilgenberg Inc.), fire polished, and coated with Sylgard (Dow Corning, Midland, MI). The standard internal solution contained 90 mM *N*-methyl-D-glucamine fluoride, 45 mM *N*-methyl-D-glucamine chloride, 7.5 mM EGTA, 1.8 mM $MgCl_2$, 9 mM HEPES, 4 mM MgATP, 0.3 mM GTP (Tris salt), and 14 mM creatinine phosphate (Tris salt), pH 7.4. The intracellular fluoride ion may help to abolish the L-type Ca^{2+} current (Akaike et al., 1983; Carbone and Lux, 1987). The capacitance and series resistance of the whole-cell configuration were mostly 5–20 pF and 2–5 MΩ (after a typical 40–60% partial compensation), respectively. Currents were recorded at room temperature (~25°C) with an Axoclamp 200A amplifier, filtered at 2–10 kHz with four-pole Bessel filter, digitized at 20–200 μsec intervals, and stored using a Digidata-1200 analog-to-digital interface along with the pClamp software (Axon Instruments, Foster City, CA). All statistics are given as mean ± SEM.

RESULTS

Block of the low-voltage-activated Ca^{2+} current by micromolar La^{3+}

Figure 1 shows typical Ca^{2+} currents recorded from neurons in the ventroposterior nuclei of thalamus. In Figure 1, *A* and *B*, the cell contains a significant amount of sustained Ca^{2+} currents, which is much more manifest with a test pulse of −10 mV than of −40 or −70 mV (i.e., high-voltage-activated) and is not very sensitive to a holding potential change from −120 to −80 mV. In contrast, the Ca^{2+} currents in the other cell (Fig. 1*C–E*) consist almost exclusively of transient currents. The transient currents are significantly activated with test pulses −70 to −40 mV (low-voltage-activated) and are rapidly inactivated with a decaying time constant of 20–25 msec. These transient currents are insensitive to 1 μM nimodipine or 0.5 μM ω-conotoxin MVIIC, yet are very sensitive to more depolarized holding potentials. Little transient Ca^{2+} current can be recorded from the same cell when the holding potential is changed from −120 to −80 mV. The rapid inactivation, the low-voltage activation, and the sensitivity to holding potential all suggest that the chief component of these transient neuronal Ca^{2+} currents is contributed by the T-type Ca^{2+} channel (T-channels) (Carbone and Lux, 1987; Fox et al., 1987; Coulter et al., 1989). This latter cell thus is classified as type II neurons (Fig. 1, legend), which contain almost only T-channels and have negligible high-voltage-activated Ca^{2+} currents. The former cell containing significant high-voltage-activated Ca^{2+} currents is classified as type I neurons. Among the 52 cells we examined, 65% (34 of 52) are type II and 35% (18 of 52) are type I. All of the subsequent studies are performed in type II neurons.

Like in the other Ca^{2+} channels, La^{3+} is a potent blocker of T-channels, in which the dissociation constants are ~0.5 μM (in dorsal root ganglion cells; Todorovic and Lingle, 1998) and 2.5 μM (in clonal GH3 pituitary cells; Herrington and Lingle, 1992). Figure 2*A* shows that most of the rapidly inactivating current in thalamic neurons is blocked by 10 μM La^{3+}. The difference between the currents recorded in the presence and absence of 10 μM La^{3+} is the La^{3+}-sensitive current. This differential current will be used later in the other experiments when it is necessary to eliminate capacity transient and tiny contamination of any non-specific currents.

Saturation of the macroscopic inactivation rate at voltages more positive than −40 mV

Figure 3 plots the peak T-current and the decaying time constant against time. The current size and the inactivation kinetics do not show significant changes in 30 min, which is long enough for collecting most data in this study. Figure 4*A–C* examines the voltage dependence of activation as well as inactivation kinetics and the steady-state inactivation curve of T-channels. The activation phase is speeded by increasing depolarization between −80 and −10 mV. On the other hand, the inactivation kinetics are accelerated with increasing depolarization only between −80 and −40 mV, yet become saturated at more positive voltages. In terms of Scheme 1, it seems that the horizontal transitions (e.g., C to O) are voltage-dependent, yet the vertical transitions (e.g., O to OB) are voltage-independent. This is similar to the case of Na^+ channels (Bezanilla and Armstrong, 1977; Bean, 1981; Aldrich et al., 1983; Gonoi and Hille, 1987). Fast inactivation of T-channels thus probably takes the C to O to OB route to develop and gets its apparent voltage dependence from the voltage dependence of activation. The saturated inactivation time constant (~20 msec) (Fig. 4*B*) could indicate a voltage-independent O to OB rate of 50 sec^{-1}. Figure 5*A–C* demonstrates deactivating tail currents of T-channels. The deactivation kinetics (i.e., rates of the O to C transition) are accelerated exponentially from −90 to −170 mV, with an apparent voltage dependence of *e*-fold acceleration per ~30 mV hyperpolarization.

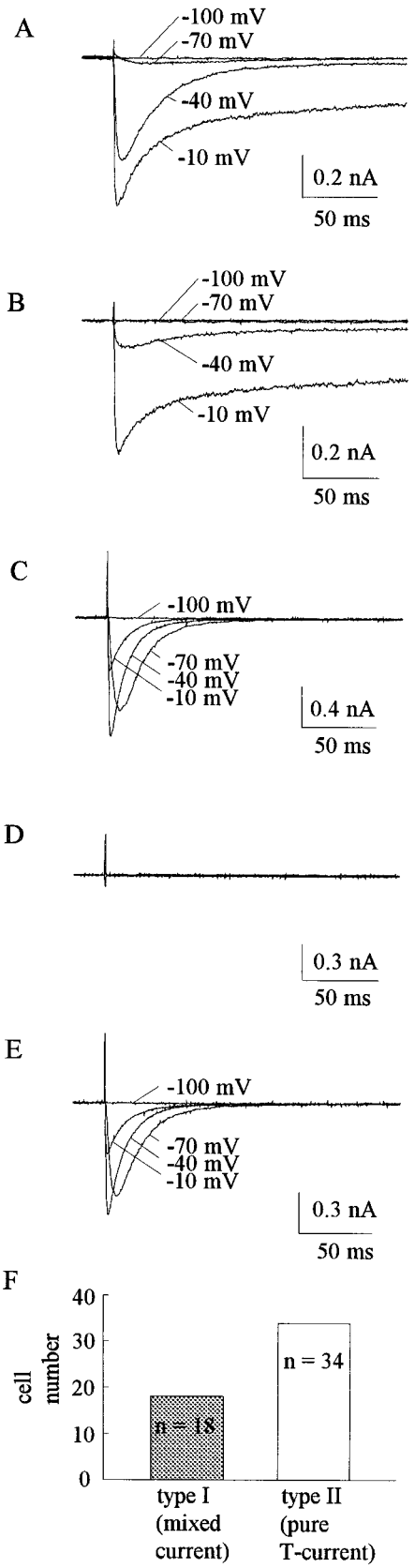

Figure 1. Two types of thalamic relay neurons with different compositions of whole-cell Ca^{2+} currents. Nimodipine and ω-conotoxin MVIIC were not added in *A–D* but were added in *E*. *A*, The cell was held at −120 mV and stepped every 5 sec to the test pulse (−100, −70, −40, and −10 mV) for 200 msec. A test pulse of −100 mV elicited no Ca^{2+} currents, which started to be discernible with a test pulse of −70 mV. At −40 mV, the Ca^{2+} currents were predominated by a rapidly inactivating or transient component (presumably T-current), whereas a more sustained component (presumably L- or N-type or other high-voltage-activated Ca^{2+} currents) became very manifest at −10 mV. *B*, The same cell and pulse protocol as that in *A*, except that the holding potential was changed to −80 mV. Note a significant decrease of the transient component but not the sustained component of the Ca^{2+} currents. *C*, The same pulse protocol as that in *A* (holding potential of −120 mV) was repeated in another cell. There was no current elicited by a test pulse of −100 mV, but significant transient current was observed with a test pulse of −70 mV. Most interestingly, no sustained current was observed with test pulses of −40 or even −10 mV. *D*, The same cell and pulse protocol as that in *C*, except that the holding potential was changed to −80 mV. No current was elicited with test pulses of −100 to −10 mV. *E*, The same cell and pulse protocol as that in *C*, except that 0.5 μM ω-conotoxin MVIIC and 1 μM nimodipine were added to the external solution. Note that the transient Ca^{2+} currents are slightly decreased in amplitude, but kinetics of the currents and the current–voltage relationship remain unchanged. *F*, The cells in which Ca^{2+} current is larger at a test pulse of −10 mV than at a test pulse of −40 mV are classified as type I neurons (typically represented by the cell in *A*). The cells in which Ca^{2+} current is smaller at a test pulse of −10 mV than at a test pulse of −40 mV are classified as type II neurons (typically represented by the cell in *C*), which always contain little discernible high-voltage-activated Ca^{2+} currents.

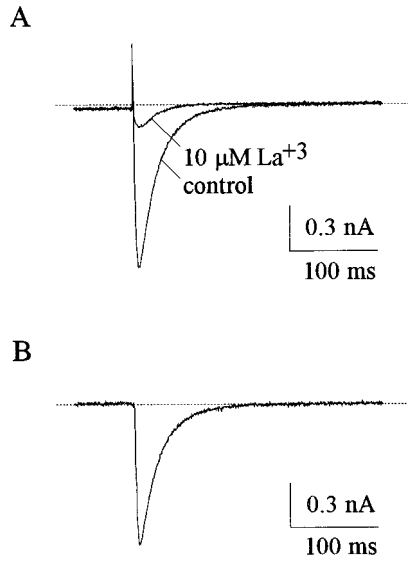

Figure 2. La^{3+} blockade of T-current. *A*, The cell was held at −120 mV and stepped every 5 sec to −50 mV for 300 msec to elicit T-current. The same pulse protocol was repeated in the presence or absence of 10 μM external La^{3+}. It is evident that 10 μM La^{3+} inhibits most of the T-current. *B*, The La^{3+}-sensitive current is obtained by subtracting the current in the presence of external La^{3+} from the current in the control external solution.

No Ca^{2+} currents associated with recovery from inactivation

If the inactivated T-channels take the OB to O to C (unblocking-first) route to recover from inactivation, there might be significant Ca^{2+} current produced by T-channels traversing the O state during the hyperpolarizing recovery pulse. On the other hand, if the inactivated T-channels take the OB to CB to C (deactivation-first) route, there would be no such Ca^{2+} current. Figure 6 shows that the latter is true not only with mildly (−80 mV) but also with more strongly (−120 mV) hyperpolarizing recovery pulses. After most T-channels are inactivated by a pulse to −40 mV, there is no discernible

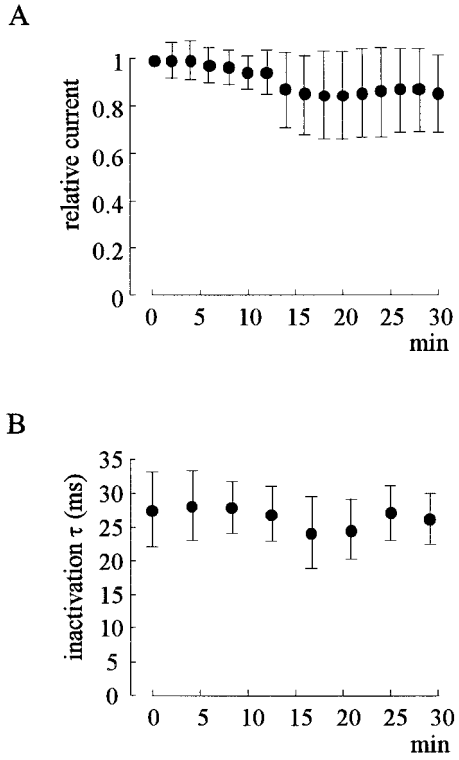

Figure 3. Insignificant rundown of T-current in 30 min. *A*, The cells were held at −120 mV, and T-current was elicited by the same pulse protocol as that in Figure 2. The peak T-currents obtained at each time point are normalized to the peak T-current of the first sweep in each cell. The mean normalized peak currents from four cells are then plotted against time. There is no significant decrease of the peak T-current in a period of 30 min. *B*, The decaying phase of the T-current in *A* is fitted by monoexponential functions, and the decaying time constant is plotted against time. The time constants show no significant change in 30 min.

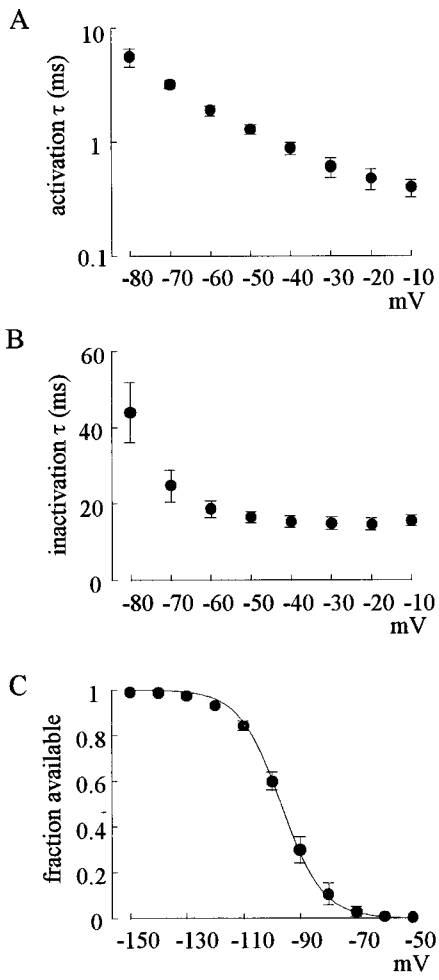

Figure 4. Voltage dependence of macroscopic activation and inactivation of T-current. *A*, The cells were held at −120 mV and stepped every 5 sec to −10 to −80 mV for 500 msec to elicit T-current. La^{3+}-sensitive currents were used to eliminate capacity transient and facilitate analysis of the currents. The rising phase of the macroscopic currents (from the beginning to the peak of each current) are fitted by monoexponential functions. The time constants from the fits are 5.6 ± 1.0, 3.2 ± 0.2, 1.9 ± 0.2, 1.3 ± 0.1, 0.89 ± 0.11, 0.61 ± 0.08, 0.48 ± 0.1, and 0.40 ± 0.07 msec for step potentials −80, −70, −60, −50, −40, −30, −20, and −10 mV, respectively (all $n = 4$; note that the *vertical axis* is in logarithmic scale). *B*, The decaying phase of the current sweeps in *A* are also fitted by monoexponential functions, and the time constants are 43.9 ± 8.0, 24.9 ± 4.2, 18.8 ± 2.3, 16.7 ± 1.7, 15.5 ± 1.2, 15.0 ± 0.8, 14.8 ± 0.8, and 15.7 ± 0.9 msec for step potentials −80, −70, −60, −50, −40, −30, −20, and −10 mV, respectively. *C*, A representative inactivation curve of T-channels from four type II thalamic neurons. The cells are held at −120 mV and stepped every 5 sec to the inactivating pulse (−50 to −150 mV) for 500 msec. The channels that remained available after each inactivating pulse were assessed by the peak currents during a following short pulse to −50 mV for 500 msec. The fraction available is defined as the normalized peak current (relative to the peak current evoked with an inactivating pulse at −150 mV) and is plotted against the voltage of the inactivating pulse. The line is a fit to the data with a Boltzmann function: fraction available $= 1/(1 + \exp((V + 96.8)/7.3))$, where V denotes the voltage of the inactivating pulse in millivolts.

current during the following hyperpolarization phase to either −80 or −120 mV. This finding suggests that inactivated T-channels take the deactivation-first route to recover, regardless of the recovery potential.

Gradual shortening of the initial delay with increasing hyperpolarization

If inactivated T-channels take the deactivation-first route to recover, then there may be an initial delay corresponding to the OB to CB step in the time course of recovery. Figure 7, *A* and *B*, shows that there is indeed an initial delay in the recovery course of inactivated T-channels in thalamic neurons. Moreover, the delay gets shorter with increasing hyperpolarization of the recovery pulse (down to −200 mV), showing an apparent voltage dependence of *e*-fold shortening per 43 mV hyperpolarization (Fig. 7*C*). The voltage dependence of the delay suggests involvement of charge movements in the pathway leading to the channel conformation from which the inactivating peptide unbinds. If the channel increases its affinity for the inactivating peptide as a result of the forward movement of the voltage sensors (i.e., channel activation), it is likely that backward movements of the sensors, or deactivation, would decrease the affinity of the blocking peptide and facilitate the unbinding process. This is qualitatively similar to the case of Na^+ channels (Kuo and Bean, 1994) and is consistent with the view that the initial delay results from deactivation of the inactivated channels. The initial delay in T-channels, however, is quantitatively very different from that in Na^+ channels, especially when taking the deactivating kinetics into consideration (see Discussion).

Saturation of the exponential phase of recovery at −100 mV

After the initial delay, the following time course of recovery can be fitted by a single exponential function (Fig. 8*A*). The recovery

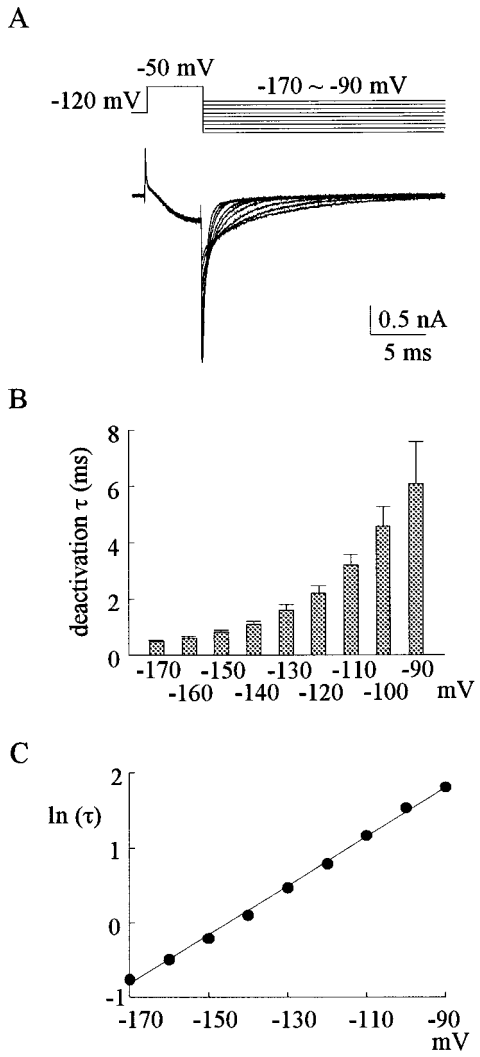

Figure 5. Voltage dependence of macroscopic deactivation of T-current. *A*, The cell was held at −120 mV and stepped every 5 sec to −50 mV for 5 msec (the activating pulse) and then to −90 to −170 mV for 30 msec (the deactivating pulse). La^{3+}-subtracted currents were used to eliminate capacity transients and facilitate subsequent fitting procedures. The tail currents show larger amplitude and faster decaying kinetics as the deactivating pulse goes more negative. *B*, The decaying phase of tail current is fitted by monoexponential functions. The decaying time constants are 6.1 ± 1.5, 4.6 ± 0.7, 3.2 ± 0.4, 2.2 ± 0.3, 1.6 ± 0.2, 1.1 ± 0.1, 0.81 ± 0.07, 0.61 ± 0.06, and 0.47 ± 0.04 msec for deactivating potentials −90, −100, −110, −120, −130, −140, −150, −160, and −170 mV, respectively (all $n = 5$). *C*, The mean value of time constant in *B* is plotted against the voltage of the deactivating pulse in a semilogarithm scale (the *longitudinal axis* is the natural logarithm of the deactivating time constant in milliseconds). The line is a linear fit of the form: $ln(\tau) = 4.77 + 0.033V$, where V denotes voltage of the deactivating pulse in millivolts.

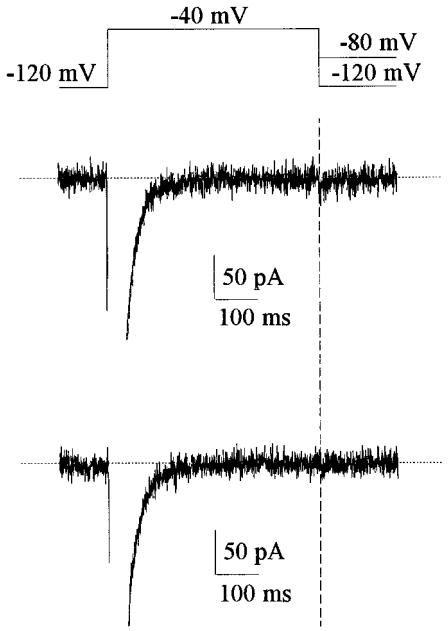

Figure 6. Lack of discernible current during the recovery phase of inactivated T-channels. The cell was held at −120 mV and stepped to −40 mV for 500 msec (the inactivating pulse) and then stepped back to −80 mV (*top*) or −120 mV (*bottom*) to recover the inactivated T-channels. La^{3+}-subtracted currents are used to eliminate contamination from leak or other nonspecific currents. No matter that the recovery potential is −80 or −120 mV, there is no discernible ionic current associated with recovery of the inactivated T-channels.

rate (reciprocal of the time constant from the exponential fit) shows no apparent voltage dependence and remains ~3.5 sec^{-1} between −100 and −200 mV (Fig. 8*B*). The mean recovery rate at −90 mV is also in the same range, but there is more variability of the data than those at the other voltages (Fig. 8*B*, larger error bar at −90 mV). The increased variability at −90 mV may be ascribable to the small recovered current, which is usually no more than 20% of the control current in pulse 1 and is always only a few tens of picoamperes in amplitude. It is therefore hard to conclude whether the recovery rate at −90 mV (the most positive among the feasible recovery potentials) is the same as the recovery rates at more negative potentials or whether it is actually slower than the saturated recovery rate, like the cases in fibroblasts or in cloned α1G T-type channels (Chen and Hess 1990; Serrano et al., 1999) (but see Herrington and Lingle, 1992). In either case, the voltage-independent saturated recovery rate at −100 mV and more negative potentials is again qualitatively similar to but quantitatively distinct from the case of Na^+ channels, in which the saturated recovery rate is achieved only with potentials more negative than −180 mV (Kuo and Bean, 1994). Because additional hyperpolarization can no longer speed the recovery from inactivation, at saturating negative membrane potentials the channels seem to recover from a conformation with the lowest affinity to the inactivating peptide. Along with the gradually shortened initial delay with increasing hyperpolarization in Figure 7, these findings are also consistent with the foregoing notion that the horizontal transitions in Scheme 1 (e.g., OB to CB) are voltage-dependent, yet the vertical transitions (e.g., CB to C) lack intrinsic voltage dependence.

DISCUSSION

The deactivation-first route for the recovery of inactivated T-channels

We have demonstrated that the recovery time course of inactivated T-channels begins with a delay, which is shortened with increasing hyperpolarization (down to −200 mV) and is followed by an exponential phase. Also, there is no discernible Ca^{2+} current associated with recovery at −80 or −120 mV. These findings indicate that, over a wide range of recovery potentials, T-channels always take the deactivation-first route to recover from inactivation and are therefore more similar to Na^+ channels

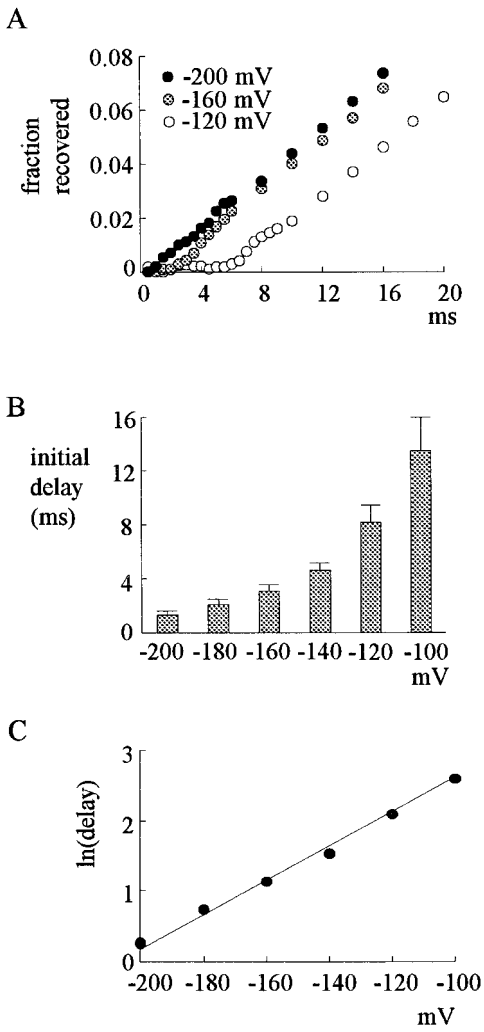

Figure 7. Initial delay in the recovery time course of T-channels over a wide range of membrane potentials. *A*, The cells was held at −120 mV and pulsed twice to −50 mV (each for 200 msec) every 6 sec, with a gradually lengthened gap between the two pulses at various potentials (the recovery potential, V_r). The average current in the last 2 msec in the first pulse is subtracted from the peak currents in both pulses to make "corrected" peak currents. The fraction of recovered channels is determined by the ratio between the corrected peak current in the second pulse and that in the first pulse. Because the fraction of recovered channels with such short V_r is very small, we try to eliminate the contamination from noises by a smoothing technique. The average value of three consecutive data points is calculated and designated as the final value of the middle point of the three and is plotted against the duration of V_r. It is evident that there is an initial delay in the recovery course with a V_r of −120 mV. The delay becomes shorter with more hyperpolarized V_r and is almost negligible with a V_r of −200 mV. Also note that the recovery courses immediately after the delay are approximately linear and are of almost identical slope with V_r of −120, −160, or −200 mV. This is consistent with the findings in Figure 8 (see below), which shows that the recovery course after the initial delay can be approximated by monoexponential functions with almost identical time constants at different *V*r. *B*, With the analysis given in *A*, if one data point is larger than its previous point, the interval between the two points is defined as an "increment." The initial delay is defined by the first data point that marks the start of four consecutive increments. The initial delays from seven to nine cells are 13.5 ± 2.5, 8.2 ± 1.3, 4.6 ± 0.6, 3.1 ± 0.5, 2.1 ± 0.4, and 1.3 ± 0.3 msec for *V*r of −100, −120, −140, −160, −180, and −200 mV, respectively. *C*, The mean value of the initial delay in *B* is plotted against *V*r in a semilogarithm scale (the *longitudinal axis* is the natural logarithm of the initial delay in milliseconds). The line is a linear fit of the form: $ln(\text{delay}) = 4.86 + 0.023V$, where V denotes V_r in millivolts.

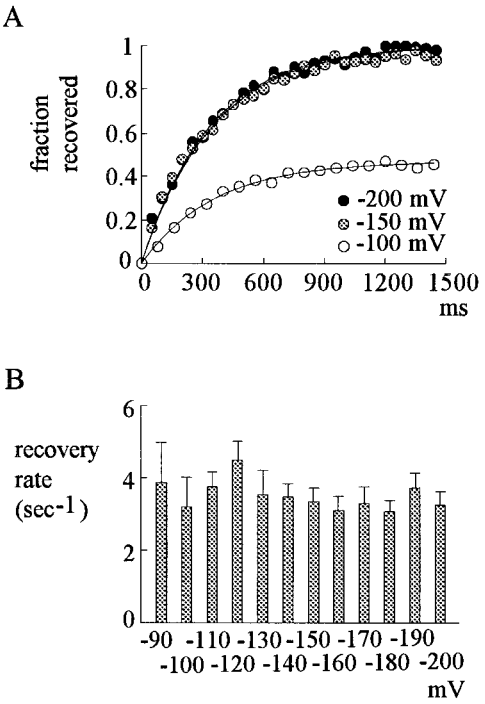

Figure 8. The exponential phase of recovery from inactivation of T-channels over a wide range of membrane potentials. *A*, Recovery of the inactivated T-channels is assessed by a similar two-pulse protocol to that in Figure 7, but here the duration of recovery gap potential (V_r) is much longer for study of the later phase of recovery. Treatment of the data with the aforementioned smoothing technique is no longer necessary because the fraction of recovered channels here is generally much larger than that obtained with the very short V_r in Figure 7. The lines are monoexponential fits of the form: fraction recovered = $0.47 - 0.47\exp(-t/353)$ (for V_r = −100 mV, and t denotes length of V_r in milliseconds; the *horizontal axis*), fraction recovered = $1 - \exp(-t/349)$ (for V_r = −150 mV), and fraction recovered = $1 - \exp(-t/340)$ (for V_r = −200 mV). *B*, The recovery rates from inactivation are given by reciprocals of the time constants from the monoexponential fits in *A*. The average results from three to six cells in each different V_r are shown.

(Kuo and Bean, 1994) than to Shaker K^+ channels (Kuo, 1997). This is interesting considering that the α subunits of T-channels and of Na^+ channels both consist of four domains (repeats) connected into one single peptide chain (Noda et al., 1986; Noda and Numa, 1987; Perez-Reyes et al., 1998), whereas a functioning Shaker K^+ channel is comprised of four α subunits (four separate peptide chains, each corresponding to one repeat in the α subunit of T-channels or Na^+ channels) (Kamb et al., 1987; MacKinnon, 1991).

Much slower binding and unbinding rates of the inactivating peptide in T-channels than in Na^+ channels

Despite of the foregoing qualitative similarity, there are significant quantitative differences between T-channels and Na^+ channels. The macroscopic rate of development of inactivation in Na^+ channels in rat hippocampal neurons saturates at ~3.5 $msec^{-1}$ at +100 mV or more positive potentials (Kuo and Bean, 1994; Kuo and Liao, 2000), whereas in thalamic neuronal T-channels, the corresponding rate saturates at ~0.07 $msec^{-1}$ at potentials as negative as −40 mV. According to Scheme 1, these data indicate a ~50-fold difference in the O to OB rate (the binding rate of the inactivating peptide) between these two channels. Moreover, in Na^+ channels the "saturated" time constant of the exponential

phase of recovery is ~4 msec^{-1}, which is achieved with very negative potentials close to −200 mV (Kuo and Bean, 1994). However, in thalamic neuronal T-channels, such a saturated rate is ~1200-fold slower (~3.5 sec^{-1}) and is obtained with much more positive potentials (e.g., −100 mV). Based on the hinged-lid model, these data suggest that both forward and backward gating movements of the inactivating peptide, namely binding to the most favorable receptor conformation in the activated channel or unbinding from the most unfavorable conformation in the deactivated channel, are much slower in T-channels than in Na^+ channels. This would raise the possibility that binding and unbinding of the inactivation peptide onto or from these channels are not free diffusion processes (which may be the case in the ball-and-chain model and Shaker K^+ channels) (Hoshi et al., 1990; Zagotta et al., 1990) but are processes controlled by conformational changes of the channel protein. The kinetic data thus suggest a much more "rigid" hinge in T-channels. (For convenience, we would discuss our data in this study with the hinged-lid model. Most discussion will remain valid and be readily translated into other terms or concepts if one prefers the other model. For example, "much more rigid hinge" would be equivalent to much greater inertia of the coupling mechanism between activation and inactivation based on more general considerations.)

Relatively small difference between binding affinity of the inactivating peptide to the activated and that to the deactivated T-channels

We have demonstrated that the recovery rate of inactivated T-channels in thalamic neurons saturates at −100 mV. Similar findings were also observed in other preparations, such as fibroblasts, clonal pituitary cells, and cloned α1G channels (Chen and Hess, 1990; Herrington and Lingle, 1992; Serrano et al., 1999). Based on Figure 9*A*, *scheme 2*, it seems that most inactivated T-channels are readily redistributed to state C1B (the fully deactivated-blocked state) at −100 mV. In this regard, it should be noted that sizable T-current is elicited by a test pulse at −70 mV (Fig. 1*C*), indicating significant distribution of unblocked T-channels to state O at this voltage. Redistribution of most unblocked T-channels to state C1 therefore would necessitate potentials more negative than −70 mV. Distribution of most blocked (inactivated) T-channels to state C1B and distribution of most unblocked T-channels to state C1 thus does not require very different potentials. This is in sharp contrast with Na^+ channels (Kuo and Bean, 1994), in which the recovery rate is saturated at −180 to −200 mV, far more negative than the voltage range at which Na^+ current starts to be significantly elicited (approximately −50 to −40 mV). The difference between the binding affinity of inactivating peptide to the activated channel and that to the fully deactivated channel thus might be quite smaller in T-channels than in Na^+ channels. This would indicate a much less drastic conformational change in the inactivation machinery (receptor, hinge, etc.) during the activation–deactivation process in T-channels.

A more abrupt conformational change in the inactivation machinery associated with opening and closing of the T-channel pore

We have noted significant distribution of unblocked T-channels to state O at −70 mV. Because of higher affinity of the inactivating peptide to the open state than to the closed state, there should be more significant or even predominant occupancy of state OB for the (blocked) inactivated T-channels at −70 mV. This is consistent with the observation that there is little recovery of T-current

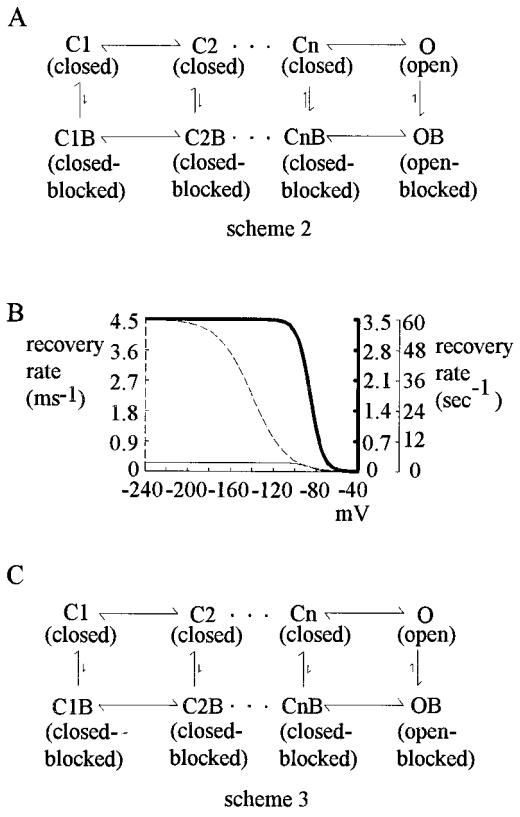

Figure 9. Gating schemes and comparison of the voltage dependence of the recovery rates between Na^+ and T-channels. *A*, *scheme 2* is a more elaborate gating diagram than Scheme 1. Depolarization moves the channel from the fully deactivated state C1 to the activated state O through intermediate closed states C2 to Cn. The binding affinity between the blocking inactivating peptide and its receptor presumably is larger if the channel is more activated (faster binding rate and slower unbinding rate toward state O, represented by the size of the *vertical arrows*). Channel inactivation is thus coupled to activation. *B*, The gradually changing recovery rate between −80 and −180 mV in Na^+ channels (the *dashed line* and the *dashed vertical axis* on the *left*) (Kuo and Bean, 1994) is ascribable to rapid redistribution of the inactivated channels among CnB to C1B during the hyperpolarizing recovery pulse. More negative potentials shift the distribution more to the left and thus increase the macroscopic recovery rate, which is saturated at approximately −200 mV when most channels are in the fully deactivated state C1B. The *dashed line* is a Boltzmann function: recovery rate (msec^{-1}) = 4.5/(1 + exp((*V* + 140)/16)), where *V* denotes the membrane potential in millivolts (the *horizontal axis*) (Kuo and Bean, 1994). In contrast, the recovery rate of inactivated T-channels in thalamic neurons saturates at much less negative potentials (approximately −100 mV; the *bold line* and the *bold vertical axis* on the *right*; also note the 1000-fold difference between the units of the *left* and *right vertical axes*). The *bold line* is a rough estimate (for the rationales underlying the derivation of the *bold line*, please refer to Discussion) and is a Boltzmann function: recovery rate (sec^{-1}) = 3.5/(1 + exp((*V* + 85)/6)), where *V* denotes the membrane potential in millivolts. The *bold line* is redrawn with a different scale (*thin line* and the *thin vertical axis* on the *right*) to demonstrate that the conformational changes represented by the *bold line* may actually be just one small part of the conformational changes represented by the *dashed line*. *C*, *scheme 3* is modified from *scheme 2* and may be a more appropriate gating diagram for T-channels. Note that the unbinding and binding rates (size of the *vertical arrows*) are unchanged among different closed states because the binding affinity of the inactivating particle toward different closed states C1 to Cn presumably does not change significantly. This scheme may well explain many key observations on T-channels in this study, including early saturation of the exponential recovery phase, apparently steeper slope of the curve describing the voltage dependence of the recovery rate, and OB to CnB transition as the rate-limiting step in the overall deactivation process of the inactivated channel.

at −80 mV or more positive potentials. Along with the saturated recovery rate at −100 mV, we propose possible voltage-dependence of the recovery rate of T-channels in Figure 9*B* (*bold line*). It is interesting to note that the curve has a steeper slope than that of the Na^+ channel (*dashed line*) (Kuo and Bean, 1994) and that of the inactivation curve in Figure 4*C*. Because distribution of channels between C1B and OB is unlikely to involve more charges than distribution between C1 and OB, the apparently steeper slope would suggest involvement of fewer intermediate states (in terms of different unbinding rates of the inactivating peptide) in the distribution of T-channels between C1B and OB. In other words, T-channels may have significantly less gradual changes of the inactivation machinery during the activation–deactivation processes than Na^+ channels.

The initial delay is still shortened with increasing hyperpolarization (Fig. 7*A*,*B*), whereas the exponential phase is saturated. Mechanistically, the delay means the average time the channel in state OB has to spend before it reaches the state at which the inactivating peptide could readily unbind. The delay therefore may serve as an indicator of the deactivation kinetics of inactivated T-channels. It is interesting that the decaying kinetics of the tail current, which presumably represents deactivation of the unblocked channels or the O to Cn transition (Fig. 9*A*), show a similar voltage dependence (0.8 equivalent charges) (Fig. 5*B*) to that of the initial delay (deactivation of the blocked channels, 0.6 equivalent charges) (Fig. 7*C*). Moreover, the decaying time constant of the tail T-current is ~4.6 msec at −100 mV. Because of higher affinity of the inactivating peptide to the O state, OB to CnB rate (Fig. 9*A*) should be slower. If this is not the rate-limiting step in the overall transition from OB to C1B, there must be other slower steps between CnB and C1B. This would be difficult to reconcile with an initial delay of only ~13.5 msec at −100 mV (Fig. 7*B*). In contrast, the deactivating tail current has a time constant of only ~0.12 msec at −100 mV in Na^+ channels (6°C, deactivation of Na^+ channels is too fast to measure at 25°C), yet the initial delay of recovery is ~6 msec in the same condition (Kuo and Bean, 1994). OB to CnB transition thus is probably the slowest, rate-limiting step in the entire deactivation process of inactivated T-channels (but not necessarily so in Na^+ channels) and thus might involve the most significant conformational change of the inactivation machinery in the activation–deactivation process. If after the rate-limiting deactivation step the inactivated T-channel always recover with the same speed (at −100 mV or more negative potentials) and if there are indeed fewer intermediate deactivated states of the inactivated T-channel, the conformational change of the inactivation machinery associated with channel activation–deactivation may not be significant until pore opening or closing in T-channels (Fig. 9*C*). This relatively "abrupt" change seems to represent just one part of what happens in Na^+ channels, in terms of both the total amount of change and the coupling mechanism of inactivation to each individual molecular step of activation.

Physiological implications

Thalamic relay neurons generate action potentials in two very different modes, the relay mode and the burst mode (Llinás and Jahnsen, 1982; McCormick and Feeser, 1990). T-channels have been implicated to play an important role in the switch between the two modes (Jahnsen and Llinás, 1984; Coulter et al., 1989; Huguenard and Prince, 1992). The burst mode prevails at more hyperpolarized basal membrane potentials that make many T-channels available, so that enough T-channels could be activated by mild depolarization to further depolarize the membrane to the threshold of firing bursts of Na^+ spikes. At more depolarized basal membrane potentials, most T-channels are inactivated and the spontaneous repetitive bursts of discharge can no longer be sustained. The neuron then responds more faithfully to external stimuli with single spike activities (the relay mode). The foregoing slow kinetics of redistributing T-channels into and out of the inactivated state thus might put important constraints on the switch between the burst and the relay modes. It would require a potential change lasting for at least a few tens of milliseconds, or preferably a few hundred milliseconds, to make the switch. This is especially so when the membrane is hyperpolarized and many inactivated T-channels are recovered through the CB to C pathway. This is probably part of the reason why duration of the IPSP in thalamic relay neurons, especially the more long-lasting late hyperpolarization produced by $GABA_B$ response, appears to play an essential role in timing the spontaneous oscillation (Jahnsen and Llinás, 1984; Hirsch and Burnod, 1987; Crunelli and Leresche, 1991; Bal et al., 1995). If T-channels had as fast kinetics as those of Na^+ channels, then even a very transient perturbation of the membrane potential might lead into modal switch. The relative slow kinetics of T-channels in thalamic neurons thus might be viewed as a built-in molecular design that helps to stabilize the different physiological presentations of the thalamocortical oscillation system.

REFERENCES

Akaike N, Nishi K, Oyama Y (1983) Characteristics of manganese current and its comparison with currents carried by other divalent ions in snail soma membranes. J Membr Biol 76:289–297.

Aldrich RW, Corey DP, Stevens CF (1983) A reinterpretation of mammalian sodium channel gating based on single channel recording. Nature 306:436–441.

Armstrong CM (1981) Sodium channels and gating currents. Physiol Rev 61:644–683.

Armstrong CM, Bezanilla F (1977) Inactivation of the sodium channel. II. Gating current experiments. J Gen Physiol 70:567–590.

Bal T, von Krosigk M, McCormick DA (1995) Role of the ferret perigeniculate nucleus in the generation of synchronized oscillations *in vitro*. J Physiol (Lond) 483:665–685.

Bean BP (1981) Sodium channel inactivation in the crayfish giant axon. Biophys J 35:595–614.

Bezanilla F, Armstrong CM (1977) Inactivation of the Na^+ channel. I. Sodium current experiments. J Gen Physiol 70:549–566.

Carbone E, Lux HD (1987) Kinetics and selectivity of a low-voltage-activated calcium current in chick and rat sensory neurons. J Physiol (Lond) 386:547–570.

Chen C, Hess P (1990) Mechanism of gating of T-type calcium channels. J Gen Physiol 96:603–630.

Coulter DA, Huguenard JR, Prince DA (1989) Calcium currents in rat thalamocortical relay neurons: kinetic properties of the transient, low-threshold current. J Physiol (Lond) 414:587–604.

Crunelli V, Leresche N (1991) A role for GABA-B receptors in excitation and inhibition of thalamocortical cells. Trends Neurosci 14:16–21.

Fox AP, Nowycky MC, Tsien RW (1987) Kinetic and pharmacological properties distinguishing three types of calcium currents in chick sensory neurons. J Physiol (Lond) 394:149–172.

Gonoi T, Hille B (1987) Gating of Na^+ channels. Inactivation modifiers discriminate among models. J Gen Physiol 89:253–274.

Herrington J, Lingle C (1992) Kinetic and pharmacological properties of low voltage activated Ca^{2+} current in rat clonal (GH3) pituitary cells. J Neurophysiol 68:213–232.

Hirsch JC, Burnod Y (1987) A synaptically evoked late hyperpolarization in the rat dorsolateral geniculate neurons *in vitro*. Neuroscience 23:457–468.

Hoshi T, Zagotta WN, Aldrich RW (1990) Biophysical and molecular mechanisms of Shaker potassium channel inactivation. Science 250:533–538.

Huguenard JR, Prince DA (1992) A novel T-type current underlies prolonged Ca^{2+}-dependent burst firing in GABAergic neurons of rat thalamic reticular nucleus. J Neurosci 12:3804–3817.

Jahnsen H, Llinás R (1984) Electrophysiological properties of guinea-pig thalamic neurons: an *in vitro* study. J Physiol (Lond) 349:105–226.

Kamb A, Iverson LE, Tanouye MA (1987) Molecular characteriza-

tion of Shaker, a *Drosophila* gene that encodes a potassium channel. Cell 50:405–413.
Kuo C-C (1997) Deactivation retards recovery from inactivation in Shaker K^+ channels. J Neurosci 17:3436–3444.
Kuo C-C, Bean BP (1994) Na^+ channels must deactivate to recover from inactivation. Neuron 12:819–829.
Kuo C-C, Liao S-Y (2000) Facilitation of recovery from inactivation by external Na^+ and location of the activation gate in neuronal Na^+ channels. J Neurosci 20:5639–5646.
Llinás R, Jahnsen H (1982) Electrophysiology of mammalian thalamic neurons *in vitro*. Nature 297:406–408.
MacKinnon R (1991) Determination of the subunit stoichiometry of a voltage-activated potassium channel. Nature 350:232–235.
McCormick DA, Bal T (1997) Sleep and arousal: thalamocortical mechanisms. Annu Rev Neurosci 20:185–215.
McCormick DA, Feeser HR (1990) Functional implications of burst firing and single spike activity in lateral geniculate relay neurons. Neuroscience 39:103–113.
Noda M, Numa S (1987) Structure and function of sodium channel. J Recept Res 7:467–497.
Noda M, Ikeda T, Kayano T, Suzuki H, Takeshima H, Takahashi T, Kuno M, Numa S (1986) Expression of functional sodium channels from cloned cDNA. Nature 322:826–828.
Perez-Reyes E, Cribbs LL, Daud A, Lacerda AE, Barclay J, Williamson MP, Fox M, Rees M, Lee J-H (1998) Molecular characterization of a neuronal low-voltage-activated T-type calcium channel. Nature 391:896–900.
Satin J, Cribbs LL (2000) Identification of a T-type Ca^{2+} channel isoform in murine atrial myocytes (AT-1 cells). Circ Res 86:636–642.
Serrano JR, Perez-Reyes E, Jones SW (1999) State-dependent inactivation of the α1G T-type calcium channel. J Gen Physiol 114:185–201.
Todorovic SM, Lingle CJ (1998) Pharmacological properties of T-type Ca^{2+} current in adult sensory neurons: effect of anticonvulsant and anesthetic agents. J Neurophysiol 79:240–252.
West JW, Patton DE, Scheuer T, Wang Y, Goldin AL, Catteral WA (1992) A cluster of hydrophobic amino acid residues required for fast Na^+ channel inactivation. Proc Natl Acad Sci USA 89:10910–10914.
Zagotta WN, Hoshi T, Aldrich RW (1990) Restoration of inactivation in mutant Shaker potassium channels by a peptide derived from ShB. Science 250:568–571.